

Continuous-wave versus pulse regime in a passively mode-locked laser with a fast saturable absorber

J. M. Soto-Crespo

Instituto de Óptica, Consejo Superior de Investigaciones Científicas, Serrano 121, 28006 Madrid, Spain

N. Akhmediev

Optical Sciences Centre, Research School of Physical Sciences and Engineering, Institute of Advanced Studies, Australian National University, Australian Capital Territory 0200, Australia

G. Town

School of Electrical and Information Engineering (J03), University of Sydney, New South Wales, 2006, Australia

(Received February 27, 2001; revised manuscript received August 15, 2001)

The phenomenon of modulation instability of continuous-wave (cw) solutions of the cubic–quintic complex Ginzburg–Landau equation is studied. It is shown that low-amplitude cw solutions are always unstable. For higher-amplitude cw solutions, there are regions of stability and regions where the cw solutions are modulationally unstable. It is found that there is an indirect relation between the stability of the soliton solutions and the modulation instability of the higher-amplitude cw solutions. However, there is no one-to-one correspondence between the two. We show that the evolution of modulationally unstable cw's depends on the system parameters. © 2002 Optical Society of America

OCIS codes: 190.5530, 190.5940, 140.3510, 320.5540.

1. INTRODUCTION

Passive mode locking allows for the generation of self-shaped ultrashort pulses in a laser system. It has been demonstrated in a number of works that the pulses generated by mode-locked fiber lasers are solitons.^{1–4} In addition to this very important feature, the mode-locked laser is a dissipative nonlinear system that can have very rich dynamics, including not only the generation of pulses of accurate shape but also much more complicated behavior. The approach that uses the complex Ginzburg–Landau equation (CGLE) in relation to passively mode-locked lasers was pioneered by Haus.⁵ It is now used extensively to describe pulse behavior in solid-state or fiber-based passively mode-locked lasers,^{6–9} optical parametric oscillators,¹⁰ free electron laser oscillator,¹¹ etc. The CGLE has also been used to describe transverse soliton effects in wide-aperture lasers.^{12–17} The reason is that the CGLE is the equation of minimum complexity that nonetheless includes the most important effects that are present in any active optical system. Various short-pulse laser designs result in a similar master equation.^{18,19} In the case of fast saturable absorbers with response times much faster than the pulse duration, the main features of pulse generation can be described by the cubic–quintic CGLE. The quintic terms in the equation are essential to ensure that pulses are stable.²⁰

This continuous model takes into account the major physical effects occurring in a laser cavity, such as dispersion, self-phase modulation, spectral filtering, and gain/

loss (both linear and nonlinear). Some delicate balances between them give rise to the majority of the effects observed experimentally. On the other hand, we assume that relaxation times do not enter explicitly into the master equation. This is possible when the pulse duration is much shorter than the relaxation times in the system, relative to both the gain medium and the saturable absorber. This condition excludes, for example, lasers that use a semiconductor Bragg reflector as a saturable absorber.^{4,21,22} We also exclude the influence of gain depletion on pulse generation.^{22,23} However, the CGLE allows us to describe a large range of solid-state and fiber lasers and serves as a basic model in laser theory.

One of the key issues in the theory of passively mode-locked lasers is the self-starting condition. There are various approaches to the problem of self-starting.^{24–26} They depend on the type of laser, and, in particular, on the type of mode locking. One of the models for self-starting is the transition from continuous-wave (cw) operation to steady-state mode-locked operation.²⁶ It has been suggested²⁷ that such a transition occurs through the modulational instability of cw solutions. One of the motivations of the present research is to make a detailed study of this possibility, based on solutions of the complex Ginzburg–Landau equation. In particular, we need to know when cw solutions of the CGLE become unstable and whether the soliton solutions are stable for the same set of parameters. The crucial question is, are the conditions for stability of cw's and solitons somehow related?

Of course, the modulation instability is not the only way of self-starting.^{24,25} However, a clear understanding of the self-starting phenomenon requires a careful study of each model. Hence here we concentrate on the question raised above.

In particular, we carefully consider both cw and soliton regimes of passively mode-locked lasers. To be specific, in studying the stability properties of cw and soliton solutions of the cubic–quintic CGLE, we have found that, although the stability properties of the two are related, there is no one-to-one correspondence between them. Modulation instability of the cw's does not necessarily lead to pulse generation. Various possibilities of cw evolution are possible, depending on the parameter values of the laser system. Only at certain values of the parameters does modulation instability of a cw solution lead to the generation of solitons.

In the optical context the cubic–quintic CGLE has the following form²⁸:

$$i\psi_z + \frac{D}{2}\psi_{tt} + |\psi|^2\psi + \nu|\psi|^4\psi \\ = i\delta\psi + i\epsilon|\psi|^2\psi + i\beta\psi_{tt} + i\mu|\psi|^4\psi, \quad (1)$$

where z is the cavity round-trip number, t is the retarded time, ψ is the normalized envelope of the field, D is the group-velocity dispersion coefficient with $D = \pm 1$ depending on whether the group-velocity dispersion is anomalous or normal, respectively, δ is the linear gain–loss coefficient, $i\beta\psi_{tt}$ account for spectral filtering or linear parabolic gain ($\beta > 0$), $\epsilon|\psi|^2\psi$ represents the nonlinear gain (which arises, e.g., from saturable absorption), the term with μ represents, if negative, the saturation of the nonlinear gain, and the one with ν corresponds, also if negative to the saturation of the nonlinear refractive index.

An important question is that of the correspondence between the equation and laser parameters. As we do not specify a particular type of laser, our theory allows us to find dimensionless parameters in Eq. (1), where cw and soliton solutions exist and can be compared. We have made this comparison over a wide range of the parameter values. To apply the theory to any particular experimental case would require certain adjustments. However, the latter is beyond our aims.

2. STATIONARY SOLUTIONS

Equation (1) has both soliton and cw stationary solutions. We ignore fronts, sinks, and sources that are beyond our interest here. To study the interrelation between the cw's and solitons, we carry out the following analysis. We reduce Eq. (1) to a set of ordinary differential equations (ODEs). Namely, we look for solutions in the form

$$\psi(t, z) = \psi_0(\tau)\exp(-i\omega z) = a(\tau)\exp[i\phi(\tau) - i\omega z], \quad (2)$$

where a and ϕ are real functions of $\tau = t - \nu z$, ν is the pulse inverse velocity, and ω is the nonlinear shift of the propagation constant. Substituting Eq. (2) into Eq. (1),

we obtain an equation for two coupled functions, a and ϕ . Separating real and imaginary parts, we get the following set of two ODEs:

$$\left[\omega - \frac{D}{2}\phi'^2 + \beta\phi'' + \nu\phi' \right] a + 2\beta\phi'a' + \frac{D}{2}a'' \\ + a^3 + \nu a^5 = 0, \\ \left(-\delta + \beta\phi'^2 + \frac{D}{2}\phi'' \right) a + (D\phi' - \nu)a' \\ - \beta a'' - \epsilon a^3 - \mu a^5 = 0, \quad (3)$$

where each prime denotes a derivative with respect to τ . It can be transformed into

$$\left(\omega - \frac{D}{2}M^2 + \beta M' + \nu M \right) a + 2\beta M a' + \frac{D}{2}a'' \\ + a^3 + \nu a^5 = 0, \\ \left(-\delta + \beta M^2 + \frac{D}{2}M' \right) a + (DM - \nu)a' \\ - \beta a'' - \epsilon a^3 - \mu a^5 = 0, \quad (4)$$

where $M = \phi'$ is the instantaneous frequency.

Separating derivatives, we obtain

$$M' = - \frac{y(8\beta^2 M + 2M - 2D\nu)}{a(4\beta^2 + 1)} \\ - \frac{4\beta\omega + 4\beta M\nu - 2\delta D}{1 + 4\beta^2} \\ + \frac{a^2(2D\epsilon - 4\beta)}{1 + 4\beta^2} + \frac{a^4(2D\mu - 4\beta\nu)}{1 + 4\beta^2}, \\ y' = M^2 a - \frac{2(D\omega + 2\beta\delta)}{1 + 4\beta^2} a - \frac{2(D + 2\beta\epsilon)}{1 + 4\beta^2} a^3 \\ - \frac{2(D\nu + 2\beta\mu)}{1 + 4\beta^2} a^5 - \frac{4\beta\nu}{1 + 4\beta^2} y - \frac{2D\nu}{1 + 4\beta^2} M a, \\ a' = y. \quad (5)$$

This set contains all stationary and uniformly translating solutions. The parameters ν and ω are the eigenvalues of Eq. (5). Pulse solutions exist only at certain values of ν and ω .

If we are only interested in zero-velocity ($\nu = 0$) solutions, Eqs. (5) can be further simplified:

$$M' = \frac{y(8\beta^2 M + 2M)}{a(4\beta^2 + 1)} - \frac{4\beta\omega - 2\delta D}{1 + 4\beta^2} + \frac{a^2(2D\epsilon - 4\beta)}{1 + 4\beta^2} + \frac{a^4(2D\mu - 4\beta\nu)}{1 + 4\beta^2},$$

$$y' = M^2 a - \frac{2(D\omega + 2\beta\delta)}{1 + 4\beta^2} a - \frac{2(D + 2\beta\epsilon)}{1 + 4\beta^2} a^3 - \frac{2(D\nu + 2\beta\mu)}{1 + 4\beta^2} a^5,$$

$$a' = y. \quad (6)$$

This set of three coupled first-order ODEs can be solved numerically. For localized solutions with correctly chosen ω , the amplitude a should go exponentially to zero outside the region of localization. Only the value of ω plays a role of an eigenvalue in this nonlinear problem. It is fixed for a given solution, but other solutions have different values of ω unless there is a degeneracy.

3. CONTINUOUS WAVES

Equations (6) have singular points defined by $M' = 0$, $y' = 0$, and $a' = 0$. The obvious one is at the origin: $a = 0$, $M = 0$. Others can be found by solving the polynomial equations that arise after equating the right-hand sides of Eqs. (6) to zero:

$$(D\mu - 2\beta\nu)a^4 + (D\epsilon - 2\beta)a^2 + (D\delta - 2\beta\omega) = 0,$$

$$M^2 = 2 \frac{[(D\omega + 2\beta\delta) + (D + 2\beta\epsilon)a^2 + (D\nu + 2\beta\mu)a^4]}{1 + 4\beta^2}. \quad (7)$$

These equations have a free parameter ω . The amplitude a is a continuous function of ω . There is none, one, or two singular points (a_0, M_0) in each quadrant of the plane (a, M) for every given ω . The locus of the singular points on the plane (a, M) is shown in Fig. 1(a) for three sets of equation parameters. As in the rest of the figures, we are using $D = 1$, i.e., we are in the anomalous-dispersion regime, although all the equations apply to any regime. The parameter that changes along each curve is ω . The dependence of the amplitude a on ω is shown in Fig. 1(b). The continuous curve in Fig. 1(b) represents one of the solutions of the biquadratic Eq. (7a), and the dashed curve represents the other solution.

The singular points define continuous waves. Returning to the analysis of Eqs. (6), we should notice that a trajectory on the plane (a, M) that starts at the origin can stop at a singular point, and the corresponding solution is a front. When the trajectory connects two nonzero stable singular points, the solution is either a sink or a source. As we already mentioned above, we are not interested in these solutions here.

It follows from Fig. 1(a) that below some threshold, there are two different solutions for a for each M . The

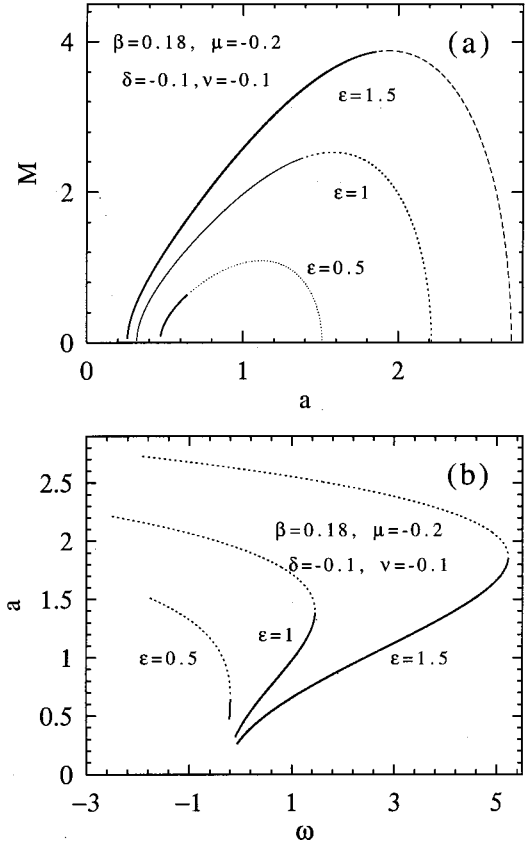


Fig. 1. (a) Locus of singular points for the set of ODEs (7). Only the upper-half for positive M is shown. The solid and the dotted curves correspond to the two solutions of the biquadratic Eq. 7(a). The equation parameters are written inside the figure. D , as in the rest of the figures, is taken to be $D = 1$. The values β , μ , ν , and δ are common for all three curves, and ϵ is different. (b) Parametric dependence of a versus ω .

minimum and the maximum values of the amplitude a take place at $M = 0$. We refer to these two values of a as low-amplitude ($a = a_1$) and high-amplitude ($a = a_2$) cw's respectively. For $M = 0$ the two cw solutions adopt the simple form

$$\psi(t, z) = a_{1,2} \exp(-i\omega z),$$

$$a_{1,2}^2 = \frac{-\epsilon \pm \sqrt{\epsilon^2 - 4\delta\mu}}{2\mu},$$

$$\omega = -\nu a^4 - a^2. \quad (8)$$

Two different values of a for each set of the equation parameters exist when

$$\epsilon^2 > 4\delta\mu. \quad (9)$$

At smaller values of ϵ there are no cw solutions. We should keep in mind, though, that there is always a trivial solution $a = 0$.

Inequality (9) means that the cubic gain must be strong enough to compensate the linear and quintic losses. The condition for the existence of soliton solutions is even stronger as the cubic gain in addition must compensate the losses due to the spectral-filtering term. We do not

have an exact criterion for the existence of solitons in analytic form. Nevertheless, the validity of the above guess is illustrated in Fig. 2(a), which shows the cw amplitude $a_{1,2}$ versus ϵ (dotted curve) and the peak amplitude versus ϵ for the plain soliton solutions, which from here on we refer to as single-pulse (SP) solitons. Similarly, Fig. 2(b) shows ω versus ϵ for the same solutions. The figure shows that the threshold for the existence of solitons is higher than the threshold for the existence of cw's. As in the continuous case, there are two soliton solutions for each ϵ above the threshold.

Our aim here is to investigate the stability of the cw waves. This can be done analytically in contrast to the problem of the soliton stability. The latter requires numerical simulations,²⁹ as the soliton solutions in general can be found only numerically. An exception is the limiting case of the nonlinear Schrödinger equation.³⁰ For

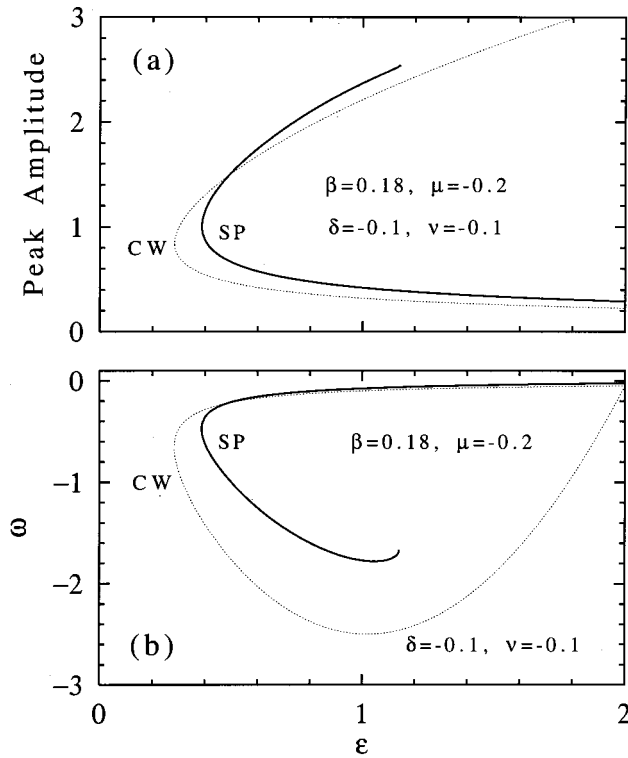


Fig. 2. (a) Cw amplitude (dotted curve) and the peak amplitude of the plain-soliton solutions (solid curve) versus ϵ . (b) ω versus ϵ for cw's and the plain-soliton solutions.

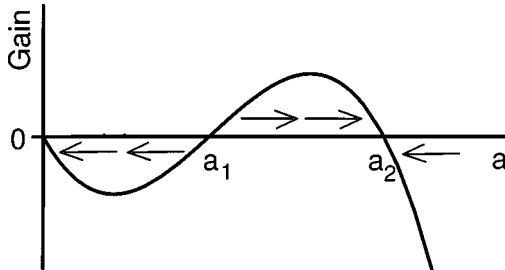


Fig. 3. Illustration of the stability for the cw solutions. The gain changes sign at the stationary values of the amplitude a . Arrows at the two intervals between the singular points show whether the amplitude at this interval increases or decreases.

cw's, simple qualitative estimates can be done on the following basis. For the background state, i.e., $\psi = 0$, to be stable, we need the condition $\delta < 0$. Additionally we need $\mu < 0$ in order for the optical field Ψ to be limited from above. Then the only positive gain term is the one with ϵ .

Stability follows from the analysis of the polynomial on the right-hand side of Eq. (1). As it is shown in Fig. 3, the value of gain changes sign at the values of cw amplitudes (a_1 and a_2). When gain is positive (between a_1 and a_2), the amplitude of the plane wave increases. When gain is negative (outside of this interval), the amplitude of the plane wave decreases. These processes are illustrated by the arrows in Fig. 3. It follows then that a cw with the amplitude a_1 is unstable, but the cw with the amplitude a_2 and trivial solution $a = 0$ are stable. However, these rough estimates do not take into account effects of modulational instability. We conclude thus that the continuous-wave solution with the higher amplitude a_2 has a chance to be stable, but the continuous-wave solution with the lower amplitude a_1 is always unstable.

We have found, from numerical simulations, that the same principle can be applied to the plain soliton solutions, which have two branches (see Fig. 2). Namely, the soliton solution with the higher amplitude has a chance to be stable whereas the soliton solution with the lower amplitude is always unstable.

4. MODULATION INSTABILITY OF CW SOLUTIONS

Continuous-wave solutions of Eq. (1) can be written in the form

$$\Psi(t, z) = a \exp[i(Mt - \omega z)], \quad (10)$$

where the variables a, M depend on ω , as Eq. (7) states. Our task here is to study modulation instability of these cw solutions. For this purpose, we add a small perturbation to solution (10):

$$\Psi(t, z) = [a \exp(iMt) + \alpha f(t, z)] \exp(-i\omega z), \quad (11)$$

where α is a small parameter and $f(t, z)$ is the perturbation function. Substituting Eq. (11) into Eq. (1) and assuming that α is small, we get the linearized evolution equation for $f(t, z)$:

$$\begin{aligned} if_z + \left(\frac{D}{2} - i\beta\right) f_{tt} + (\omega - i\delta)f + (1 - i\epsilon) \\ \times [2a^2 f + a^2 \exp(2iMt) f^*] + (\nu - i\mu) \\ \times [3a^4 + 2a^4 \exp(2iMt) f^*] = 0, \end{aligned} \quad (12)$$

where the asterisk denotes complex conjugate. This is a set of linear partial differential equations that can be solved with the standard technique of separation of variables.

We are interested in solutions of the form

$$f(t, z) = h(t, g) \exp(gz), \quad (13)$$

where g is a complex eigenvalue. The real part of g is the perturbation growth rate. For each g , the t dependence

of h is a periodic function [$\approx \exp(-i\Omega t)$] with frequency Ω . For each Fourier component, Eq. (12) results in

$$\begin{aligned} & [\omega + i(g - \delta)]\tilde{f}(\Omega) - \Omega^2 \left(\frac{D}{2} - i\beta \right) \tilde{f}(\Omega) + (1 - i\epsilon) \\ & \times [2a^2\tilde{f}(\Omega) + a^2\tilde{f}^*(2M - \Omega)] + (\nu - i\mu) \\ & \times [3a^4\tilde{f}(\Omega) + 2a^4\tilde{f}^*(2M - \Omega)] = 0. \end{aligned} \quad (14)$$

Similarly, we can write the equation for $\tilde{f}^*(2M - \Omega)$. The complex conjugate of this equation is

$$\begin{aligned} & [\omega - i(g - \delta)]\tilde{f}^*(2M - \Omega) - (2M - \Omega)^2 \\ & \times \left(\frac{D}{2} + i\beta \right) \tilde{f}^*(2M - \Omega) + (1 + i\epsilon) \\ & \times [2a^2\tilde{f}^*(2M - \Omega) + a^2\tilde{f}(\Omega)] + (\nu + i\mu) \\ & \times [3a^4\tilde{f}^*(2M - \Omega) + 2a^4\tilde{f}(\Omega)] = 0. \end{aligned} \quad (15)$$

Equations (14) and (15) are two coupled linear equations relative to the two independent functions $\tilde{f}(\Omega)$ and $\tilde{f}^*[(2M/a^2) - \Omega]$. We denote them as A_1 and A_2 . The two equations can then be written in a matrix form:

$$\begin{bmatrix} ig + C & P \\ P^* & S - ig \end{bmatrix} \begin{bmatrix} A_1 \\ A_2 \end{bmatrix} = \begin{bmatrix} 0 \\ 0 \end{bmatrix}, \quad (16)$$

where

$$\begin{aligned} C &= \omega - i\delta - \Omega^2 \left(\frac{D}{2} - i\beta \right) + (1 - i\epsilon)2a^2 \\ & \quad + (\nu - i\mu)3a^4, \\ S &= C^* - [(2M)^2 - 4M\Omega] \left(\frac{D}{2} + i\beta \right), \\ P &= (1 - i\epsilon)a^2 + (\nu - i\mu)2a^4. \end{aligned} \quad (17)$$

The existence of nontrivial solutions requires the determinant of the square matrix in Eq. (16) to be zero. This leads to the dispersion relation

$$g^2 + ig(S - C) + CS - |P|^2 = 0 \quad (18)$$

relative to the value of g . When $M = 0$, the solution is

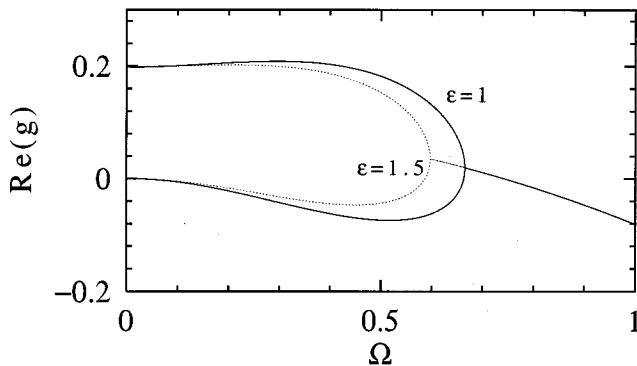


Fig. 4. Real part of the eigenvalue g as a function of the perturbation frequency Ω for the lower-amplitude cw solution. The values of the parameters are $\beta = 0.18$, $\delta = -0.1$, $\mu = -0.1$, $\nu = -0.6$, $\epsilon = 1$ (continuous curve), and $\epsilon = 1.5$ (dotted curve).

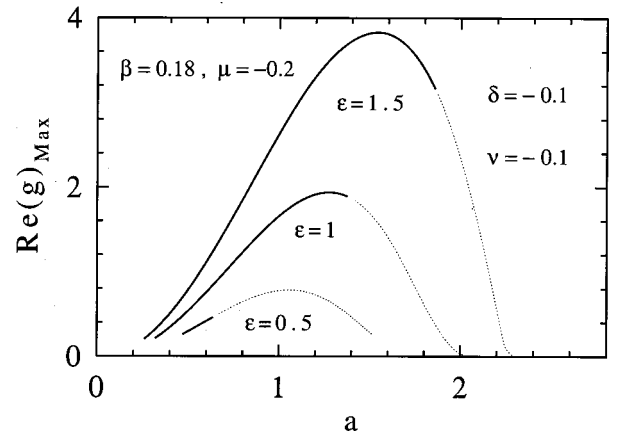


Fig. 5. Maximum growth rate as a function of a . Parameter values are $\beta = 0.18$, $\delta = -0.1$, $\mu = -0.2$, $\nu = -0.1$, and $\epsilon = 1.5$ (upper curve), 1 (middle curve), and 0.5 (lowest curve). These values of ϵ are the same as in Fig. 1.

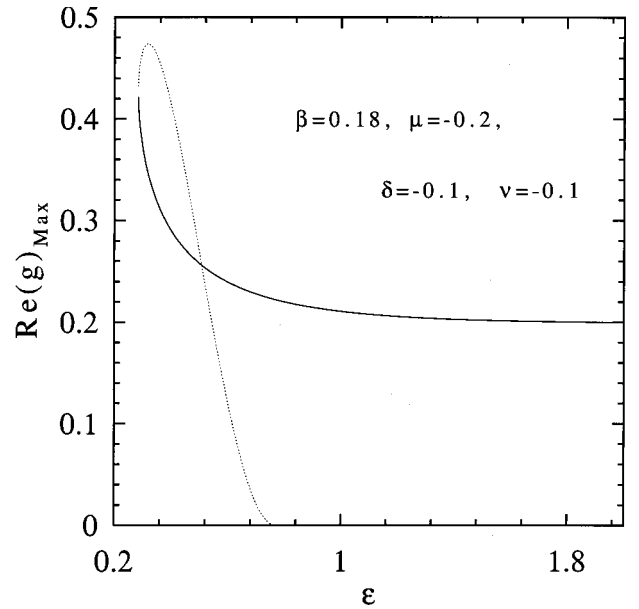


Fig. 6. Maximum growth rate, $\text{Re}(g)_{\text{max}}$, as a function of ϵ for the cw solutions with $M = 0$. The continuous curve is for the low-amplitude cw solutions, and the dotted curve is for the high-amplitude cw solutions.

$$g = -\text{Im}(C) \pm \sqrt{|P|^2 - [\text{Re}(C)]^2}, \quad (19)$$

where $\text{Re}(C)$ and $\text{Im}(C)$ denote the real and imaginary parts of C , respectively.

We have calculated g from Eq. (19) for the following set of parameters: $\beta = 0.18$, $\delta = -0.1$, $\mu = -0.1$, and $\nu = -0.6$. Figure 4 shows the real part of g versus Ω for $\epsilon = 1.5$ (dotted curve) and $\epsilon = 1$ (continuous curve) for the low-amplitude cw solutions with $M = 0$. For these equation parameters they are $\Psi(t, z) = 0.26 \exp(i 0.095z)$ ($\epsilon = 1.5$) and $\Psi(t, z) = 0.32 \times \exp(i 0.064z)$ ($\epsilon = 1$). The case shown in Fig. 4 can be considered as a generic example. The real part of the eigenvalue g splits at Ω values lower than a threshold defined by the discriminant of Eq. (18). Whenever the real part of g is positive for any value of Ω , the solution is un-

stable. As the real part of g is positive starting from zero until certain finite Ω , the cw solution is unstable relative to long-wave perturbations.

Knowing the whole function $g(\Omega)$, we can find the value of Ω where g has a maximum real part, i.e., the point where the growth rate is the highest. Examples are shown in Fig. 5 for the cw solutions that are presented in Fig. 1. Comparing the values of a in Fig. 1 with those in Fig. 5, we can see that the growth rate is positive for all small-amplitude cw solutions. However, in some cases, there are regions in the parameter space where cw solutions with the higher amplitude are stable. These results illustrate more accurately the following general principle: the cw solutions with the lower values of a are unstable, whereas those with the higher values have a chance of being stable. The two limiting cases correspond to $M = 0$. Figure 5 shows that the solutions with the higher values of a are stable at $\epsilon = 1.5$ and 1, whereas for $\epsilon = 0.5$ the whole bunch of cw solutions is unstable.

When $M = 0$, the stability of the cw solutions is determined from Eq. (19). The growth rate for this instability is shown in Fig. 6. The lower-amplitude cw solutions are unstable at every ϵ . The higher-amplitude cw solutions are unstable for $\epsilon < 0.77$ but stable above this threshold.

As we can see from Fig. 2, the soliton solutions also exist in pairs: low-amplitude and high-amplitude solitons. The stability properties of solitons are similar to those of cw's. The soliton solutions with small amplitude are always unstable, whereas the solitons with higher peak amplitude have a change to be stable. In this particular case the stability interval for solitons is [0.39, 1.016].

5. INSTABILITY OF CW VERSUS STABILITY OF SP SOLITONS

Modulation instability should create a train of pulses out of cw's when the latter is unstable. Hence intuitively one would expect to find stable solitons whenever all the cw solutions are unstable.^{26,27} We can see from the results of this section that there are some grounds for this conjecture. However, we have found that this principle is not completely correct. The following set of figures shows the relation between the stability of cw's and the stability of the upper-branch plain (SP) solitons. We specify SP solitons as plain (bell-shape) solitons. It is known that several types of soliton solutions can exist simultaneously.²⁸ Other soliton solutions with more complicated profiles exist in a smaller region of parameters and are not considered here.

The regions of stability of SP solitons can be found with a direct beam-propagation method; we use a split-step Fourier method. We took advantage of the fact²⁹ that at the values of parameters where stable solitons exist, practically any initial condition that is close enough to the soliton solution converges quickly to the SP soliton. Step by step, changing slightly the values of the equation parameters, and using as the initial condition the soliton solution from the previous step, we were able to find the regions of parameters where stable SP solitons exist. Alternatively the stability can be determined if we first find [using a shooting technique to solve Eqs. (3)] the sta-

tionary solutions and then use a Crank–Nicholson method to analyze their stability. In both cases the results are identical and are both highly computer-time-consuming tasks. For the aims of the present paper we partly used the results of our previous work.²⁹ In analyzing the cw solutions, we then choose the parameters for which the regions of stable SP solitons were previously calculated.

In fact, we studied soliton stability in the widest possible range of parameters. First, let us note that there are restrictions dictated by the underlying physics of the problem under consideration. In particular, δ must be negative in order for the background to be stable, μ must also be negative to limit the amplitudes from above, and β must be positive in order to stabilize the soliton in the frequency domain. These considerations show clearly that ϵ can be the only gain term (>0) in this model. In a way, it is responsible for the existence of any structure in this dissipative system. Hence we can consider ϵ as the most important parameter that is related to the pump.

It would be a confusing and complicated task to try to change several parameters at once. So we fixed all parameters except ϵ and one of the other parameters (either δ , μ , or ν) that were variable. All these parameters were changed in the widest possible range, covering the whole range of stability of SP solitons. The particular choice of the three fixed parameters was not critical, and we got qualitatively similar results for any other sets of these parameters. The results for both SP solitons and cw solutions are presented simultaneously in the following set of figures.

Figure 7 shows the region in the plane (δ, ϵ) where the upper cw solution is unstable and the region where the upper SP is stable. We can see clearly the similarity between the two regions. The shift of the region for stable solitons to higher values of ϵ is related to having nonzero β . The shape of this region is similar for any value of β ,

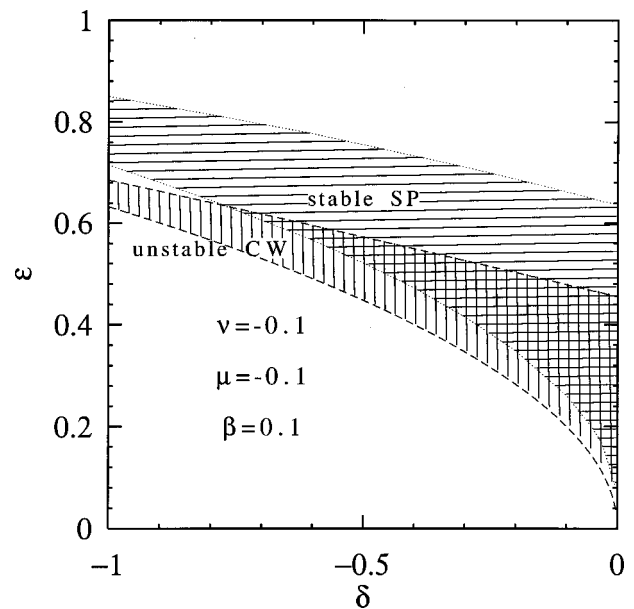


Fig. 7. Region (vertically hatched area) in the plane (δ, ϵ) where all the cw solutions are unstable and the region (horizontally hatched area) where SP solitons are stable.

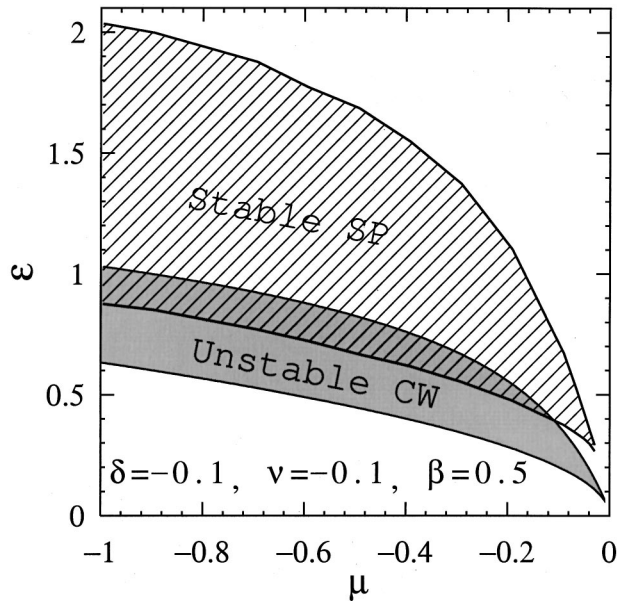


Fig. 8. Region (shaded) in the plane (μ, ϵ) where cw solutions are modulationally unstable and the region (dashed) where SP solitons are stable.

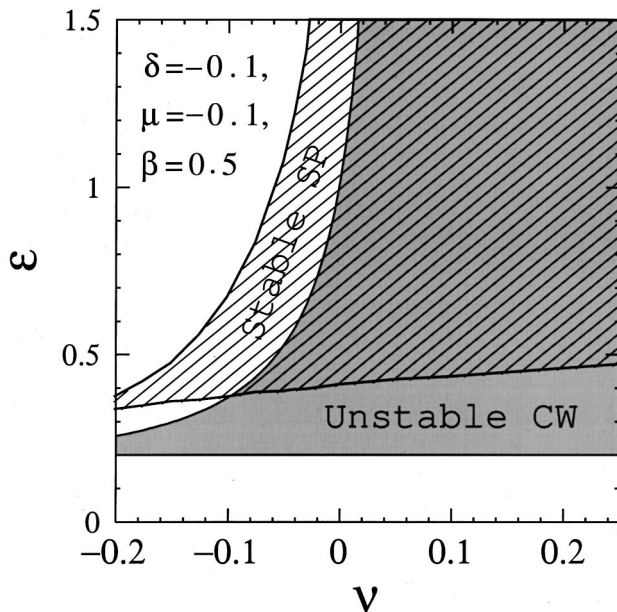


Fig. 9. Region (shaded) in the plane (ν, ϵ) where all cw solutions are modulationally unstable and the region (dashed) where SP solitons are stable.

but the region where stable pulses exist moves increasingly upward as β increases. Note that both parameters δ and ϵ change in a very wide range of values, namely, from zero to -1 or $+1$, respectively. In fact, the range where ϵ changes covers the whole region of existence for stable SP solitons. This means that our results are valid for all those cases where cw and soliton solutions exist.

Figure 8 shows the area in the plane (μ, ϵ) where the cw solutions are unstable and also the region where SP solitons are stable. The similarity between these two regions is striking, although one is shifted relative to the other due to the above-mentioned reason. Note that here the value of β is higher ($\beta = 0.5$) than in Fig. 7. Corre-

spondingly the shift between the two regions is greater in the ϵ domain. Another slice of the five-dimensional space of parameters is shown in Fig. 9. This is the (ν, ϵ) plane in the parameter space. The same striking similarity between the two regions can be noticed. In fact, in the limit of small β these two regions would almost coincide. The value of β in these simulations is relatively high so that the ϵ values differ approximately by a factor of 2. However, the two regions have a common region of overlapping. Again, we stress here that the range in which the parameters change in Figs. 8 and 9 is large. It is from zero to -1 in the case of μ and covers both negative and positive values of ν . This shows that the phenomenon we have found is quite general. It is not related to any specific choice of parameters.

At the values of the parameters where the two regions overlap, modulation instability of the cw solutions creates a train of pulses, as expected. However, if the region of unstable cw's is below the region of stable SP solitons, the cw decays without creating solitons. This example shows that self-starting of the laser is not always related to modulation instability of cw's.

To avoid any confusion, we note that the train of pulses in the t domain is not related to the round-trip time of the laser. The latter is not present in our model and is usually much longer than the distance between the pulses in the train. For reasons related to the gain depletion (which we are also ignoring here) only one (or a few) of the pulses in the train tend to survive. This indeed happens when gain depletion is explicitly taken into account.²³

6. EVOLUTION OF THE UNSTABLE CW SOLUTIONS

From Figs. 7–9 we can see that essentially there are three cases we need to study. The three examples of propagation are shown in the following figures. Our expectations are fully confirmed by numerical simulations. Figure 10 shows an example of a cw solution slightly perturbed by a single periodic wave. The initial condition is

$$\Psi(t, 0) = a + 0.001 \cos(\Omega t), \quad (20)$$

where the frequency Ω is chosen in such a way that its associated growth rate is the highest, and a is the corresponding value for the lowest-amplitude cw solution. Only one period $T = 2\pi/\Omega$ needs to be simulated. The equation parameters are $\beta = 0.18$, $\delta = -0.1$, $\mu = -0.2$, $\nu = -0.1$, and $\epsilon = 0.37$. There is no any stable-pulse solution for this case (let us recall that stable pulses exist for these values of β , δ , ν , and μ for ϵ in the interval $[0.39, 1.014]$), and as Fig. 6 shows, all the cw solutions are also unstable. Nor do any stable periodic solutions exist for these values of the parameters. The perturbation grows initially as the cw is modulationally unstable. However, after the peak evolves into a pulse, it decays, as there are no stable pulses or periodic solutions for these values of the equation parameters. Similar behavior is observed when a is the corresponding high-amplitude cw solution.

Another case of cw evolution is shown in Fig. 11. As in the previous figure, the initial condition is given by Eq. (20), where a is the lower-amplitude cw solution at ϵ

$= 1.5$, and Ω is the frequency of the perturbation with the largest growth rate. The initial stage of evolution is similar to the previous case, i.e., the cw is transformed into a train of pulses because the lower-amplitude cw is always unstable. However, either the pulses or periodic solutions at these values of the parameters are also unstable. The final result of the evolution is the transformation of the train of pulses into the high-amplitude cw which is the only stable solution.

Figure 12 shows an example of propagation when the high-amplitude cw is also unstable but the soliton solution is stable. As a result, the cw solution is transformed into a train of solitons. In our model we ignore the gain depletion. When we take it into account, only one or a few pulses will survive out of the train. Practically, this would correspond to a repetition rate related to a round-trip time rather than the periodicity of our model.

We took as the initial input the low-amplitude cw solution perturbed as Eq. (20) indicates. In this particular simulation we took Ω ten times lower than that corresponding to the largest growth rate. In this case each soliton in the train is well isolated from the others and can be considered as a single soliton. We have made several simulations with different values of Ω , and the final

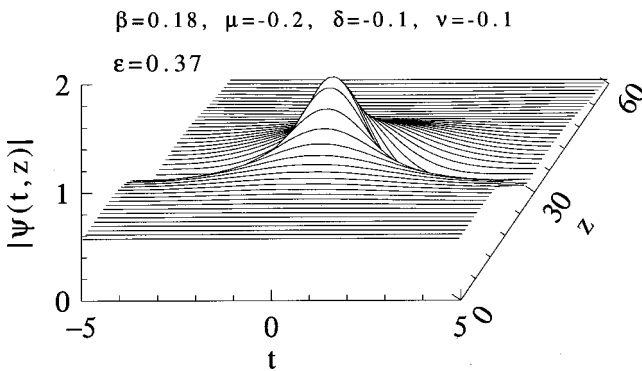


Fig. 10. Evolution of the low-amplitude cw solution perturbed by a weak periodic wave. The perturbation initially grows, but finally the whole solution vanishes because of the absence of stable pulses at these values of the equation parameters.

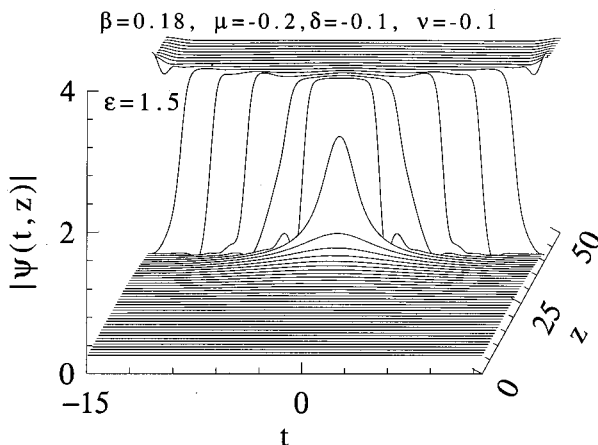


Fig. 11. Evolution of the low-amplitude cw perturbed by a weak periodic wave. The perturbation grows, and the cw is gradually transformed into the higher-amplitude cw solution, which is the only stable solution for these values of the parameters.

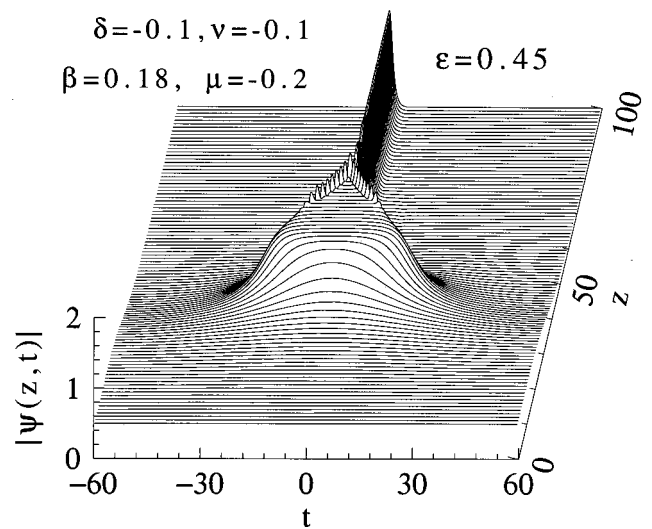


Fig. 12. Transformation of an unstable cw solution into a stable soliton. Parameter values are shown in the figure.

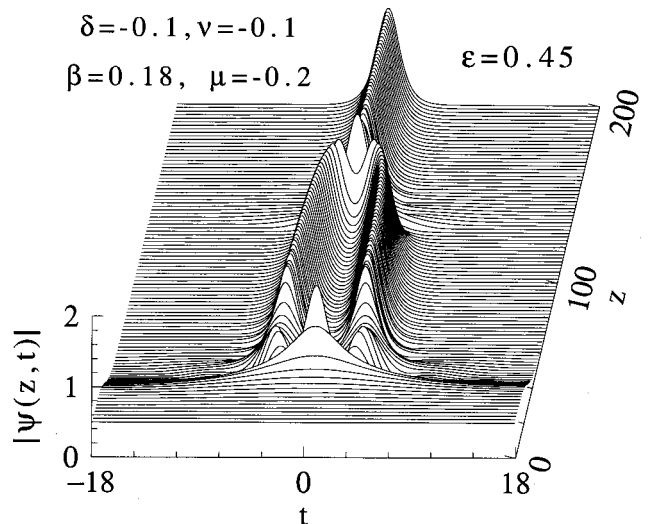


Fig. 13. Same as Fig. 12 but with a periodical perturbation of different frequency. The period of the perturbation is the length of the x axis.

result is always the one shown in this figure. In some occasions several pulses can be formed initially. This can be seen clearly in Fig. 13. However, in the result of their interaction, only one survives.

Generally, dissipative systems have a multiplicity of solutions, including periodic solutions. This is true for the CGLE as well as for more complicated systems.³¹ Competition between the periodic and localized structures³¹ is also an important problem in the case of laser systems. However, to study this competition, we have to take into account more details about the laser. In particular, we need to take into account the gain depletion, which is not included in Eq. (1).

7. CONCLUSIONS

In conclusion, we have studied the phenomenon of modulation instability of cw solutions of the cubic-quintic CGLE. We have found that low-amplitude cw solutions

are always unstable. For the high-amplitude cw solution there are regions of stability and regions of parameters where the cw solutions are modulationally unstable. We have also found that there is an indirect relation between the stability of the soliton solution and the modulation instability of the higher-amplitude cw solutions. However, there is no one-to-one correspondence between these two regions. As a result, the evolution of modulationally unstable cw's can be quite complicated. The main conclusion from our work is that the pulse operation of a passively mode-locked laser is not necessarily related to the modulation instability of the cw solutions.

ACKNOWLEDGMENTS

The authors gratefully acknowledge valuable discussions with A. Ankiewicz. The work of J. M. Soto-Crespo was supported by the Spanish Ministerio de Ciencia y Tecnología under contract BFM2000-0806 and by the Australian Research Council. N. Akhmediev and G. Town are members of the Australian Photonics Cooperative Research Centre. N. Akhmediev acknowledges support from the U.S. Army Research Office, Far East, under grant N62649-01-1-0002.

REFERENCES

- L. F. Mollenauer and R. H. Stolen, "The soliton laser," *Opt. Lett.* **9**, 13–15 (1984).
- H. A. Haus and M. N. Islam, "Theory of soliton laser," *IEEE J. Quantum Electron.* **QE-21**, 1172–1177 (1985).
- S. M. J. Kelly, "Mode-locking dynamics of a laser coupled to an empty external cavity," *Opt. Commun.* **70**, 495 (1989).
- F. X. Kärtner, I. D. Jung, and U. Keller, "Soliton mode-locking with saturable absorbers," *IEEE J. Sel. Top. Quantum Electron.* **2**, 540–556 (1996).
- H. Haus, "Theory of mode locking with a fast saturable absorber," *J. Appl. Phys.* **46**, 3049–3058 (1975).
- P. A. Belanger, "Coupled-cavity mode locking: a nonlinear model," *J. Opt. Soc. Am. B* **8**, 2077–2082 (1991).
- A. I. Chernykh and S. K. Turitsyn, "Soliton and collapse regimes of pulse generation in passively mode-locking laser systems," *Opt. Lett.* **20**, 398–400 (1995).
- F. I. Khatri, J. D. Moores, G. Lenz, and H. A. Haus, "Models for self-limited additive pulse mode-locking," *Opt. Commun.* **114**, 447–452 (1995).
- C.-J. Chen, P. K. A. Wai, and C. R. Menyuk, "Stability of passively mode-locked fiber lasers with fast saturable absorption," *Opt. Lett.* **19**, 198–200 (1995).
- P.-S. Jian, W. E. Torruellas, M. Haelterman, S. Trillo, U. Peschel, and F. Lederer, "Solitons of singly resonant optical parametric oscillators," *Opt. Lett.* **24**, 400–402 (1999).
- C. S. Ng and A. Bhattacharjee, "Ginzburg–Landau model and single-mode operation of a free-electron laser oscillator," *Phys. Rev. Lett.* **82**, 2665–2668 (1999).
- C. O. Weiss, "Spatio-temporal structures. Part II. Vortices and defects in lasers," *Phys. Rep.* **219**, 311–338 (1992).
- A. M. Dunlop, E. M. Wright, and W. J. Firth, "Spatial soliton laser," *Opt. Commun.* **147**, 393–401 (1998).
- V. B. Taranenko, K. Staliunas, and C. O. Weiss, "Spatial soliton laser: localized structures in a laser with a saturable absorber in a self-imaging resonator," *Phys. Rev. A* **56**, 1582–1591 (1997).
- W. J. Firth and A. J. Scroggie, "Optical bullet holes: robust controllable localized states of a nonlinear cavity," *Phys. Rev. Lett.* **76**, 1623–1626 (1996).
- N. N. Rozanov, *Optical Bistability and Hysteresis in Distributed Nonlinear Systems* (Physical and Mathematical Literature, Moscow, 1997).
- P. K. Jakobsen, J. V. Moloney, A. C. Newell, and R. Indik, "Space–time dynamics of wide-gain-section lasers," *Phys. Rev. A* **45**, 8129–8147 (1992).
- H. A. Haus, J. G. Fujimoto, and E. P. Ippen, "Structures for additive pulse mode locking," *J. Opt. Soc. Am. B* **8**, 2068–2076 (1995).
- E. P. Ippen, "Principles of passive mode locking," *Appl. Phys. B* **58**, 159–170 (1994).
- J. D. Moores, "On the Ginzburg–Landau laser mode-locking model with fifth-order saturable absorber term," *Opt. Commun.* **96**, 65–70 (1993).
- B. C. Collings, K. Bergman, and W. H. Knox, "True fundamental solitons in a passively mode-locked short cavity Cr⁴⁺:YAG laser," *Opt. Lett.* **22**, 1098–1100 (1997).
- F. X. Kärtner and U. Keller, "Stabilization of solitonlike pulses with a slow saturable absorber," *Opt. Lett.* **20**, 16–18 (1995).
- M. J. Lederer, B. Luther-Davies, H. H. Tan, C. Jagadish, N. N. Akhmediev, and J. M. Soto-Crespo, "Multipulse operation of a Ti:sapphire laser modelocked by an ion-implanted semiconductor saturable absorber mirror," *J. Opt. Soc. Am. B* **16**, 895–904 (1999).
- J. Hermann, "Starting dynamic, self-starting condition and mode-locking threshold in passive, coupled-cavity or Kerr-lens mode-locked solid-state lasers," *Opt. Commun.* **98**, 111–116 (1993).
- H. A. Haus and E. P. Ippen, "Self-starting of passively mode-locked lasers," *Opt. Lett.* **16**, 235–237 (1991).
- F. Krausz, T. Brabec, and Ch. Spielmann, "Self-starting passive mode-locking," *Opt. Lett.* **16**, 235–237 (1991).
- C.-J. Chen, P. K. A. Wai, and C. R. Menyuk, "Self-starting of passively mode-locked lasers with fast saturable absorbers," *Opt. Lett.* **20**, 350–352 (1995).
- N. N. Akhmediev and A. Ankiewicz, *Solitons: Nonlinear Pulses and Beams* (Chapman & Hall, London, 1997).
- J. M. Soto-Crespo, N. N. Akhmediev, and V. V. Afanasjev, "Stability of the pulslike solutions of the quintic complex Ginzburg–Landau equation," *J. Opt. Soc. Am. B* **13**, 1439–1449 (1996).
- T. Kapitula and B. Sandstede, "Instability mechanism for bright solitary-wave solutions to the cubic–quintic Ginzburg–Landau equation," *J. Opt. Soc. Am. B* **15**, 2757–2762 (1998).
- P. Couillet, C. Riera, and C. Tresser, "Stable static localized structures in one dimension," *Phys. Rev. Lett.* **84**, 3069–3072 (2000).